Phys. Lett. B 849 (2024) 138422

Contents lists available at ScienceDirect

Physics Letters B

journal homepage: www.elsevier.com/locate/physletb

Letter

A unified description of the halo nucleus ^{37}Mg from microscopic structure to reaction observables

Jia-Lin An [a,b], Kai-Yuan Zhang [c,d,*], Qi Lu [a], Shi-Yi Zhong [a], Shi-Sheng Zhang [a,*]

[a] School of Physics, Beihang University, Beijing 100191, China
[b] Baoding Hospital of Beijing Children's Hospital, Baoding, Hebei 071000, China
[c] Institute of Nuclear Physics and Chemistry, CAEP, Mianyang, Sichuan 621900, China
[d] State Key Laboratory of Nuclear Physics and Technology, School of Physics, Peking University, Beijing 100871, China

ARTICLE INFO

Editor: B. Balantekin

Keywords:
^{37}Mg
Halo
Glauber model
The DRHBc theory
Reaction cross section
Longitudinal momentum distribution

ABSTRACT

Based on the structure input directly from the deformed relativistic Hartree-Bogoliubov theory in continuum (DRHBc), we fully study reaction observables to search for halo evidence of ^{37}Mg with the Glauber model. In this scheme, we evaluate the reaction cross sections of $^{20-37}$Mg bombarding a C target at 240 MeV/nucleon and find that most of the results agree well with the experimental data within 1σ uncertainty, especially good for the case of ^{37}Mg. Our predicted doubling of the cross section change from ^{36}Mg to ^{37}Mg over that from ^{34}Mg to ^{35}Mg is consistent with a halo structure in ^{37}Mg. Additionally, our calculated narrow longitudinal momentum distribution of ^{36}Mg residues from ^{37}Mg + ^{12}C breakup agrees well with data and imply a nuclear size much larger than ^{35}Mg. Furthermore, our study shows a dominant p-wave contribution to the longitudinal momentum distribution, supporting the conclusion that ^{37}Mg is a p-wave halo nucleus. Our study provides the first unified description of the halo characteristics of ^{37}Mg from nuclear structure to reaction dynamics.

1. Introduction

An extended spatial distribution of the valence nucleon(s) in exotic nuclei has the consequence of small nucleon separation energies that make the system loosely bound [1–8]. In the breakup reactions of such exotic nuclei bombarding a C target [9,10], an increase of the interaction cross section implies a large radius of a halo nucleus. On the other hand, for a Pb target, the Coulomb breakup cross sections appear to be enhanced due to the soft $E1$ excitation [9,10]. Furthermore, a narrow momentum distribution of the residues is commonly regarded as direct evidence for a halo formation. So far, there are about 20 halo nuclei that have been suggested or confirmed from experiments since the discovery of the first case, ^{11}Li [11], in 1985. Until now, ^{37}Mg remains the heaviest halo nucleus identified as a p-wave case since 2014 [12,13].

Previously, the loosely bound valence nucleon(s) significantly occupying a low angular momentum (s or p) orbital is commonly believed to be the chief mechanism to form a halo. However, this was contradicted when a small s-wave component of $\approx 9\%$ was declared in the halo nucleus ^{17}B [14]. Due to the ambiguity of the structure mechanism and extremely low production cross sections for the most neutron-rich isotopes [15], the search for the next heavier halo nucleus is challenging, and needs an effective theoretical tool to suggest candidates. First of all, the method should appropriately describe the halo nucleus ^{37}Mg. Recently, the Facility for Rare Isotope Beams is producing isotopes in the mass region of $A \gtrsim 40$ along the neutron drip line up to argon [16], and the short lifetimes of several exotic nuclei have been measured [17,18], which may also cast a light on new halo candidates.

We briefly review the previous studies of neutron-rich magnesium isotopes. The reaction cross sections for $^{24-38}$Mg on a C target at energies around 240 MeV/nucleon have been measured precisely at the Radioactive Isotope Beam Factory at RIKEN [13]. Near the neutron drip line, the sudden enhancement of reaction cross section σ_R for ^{37}Mg has been observed. In Ref. [12], nuclear- and Coulomb-dominated one-neutron removal cross sections of ^{37}Mg on C and Pb targets were measured, respectively, together with the inclusive longitudinal momentum distribution of ^{36}Mg from ^{37}Mg on a C target. The results were used to determine a small one-neutron separation energy (S_n) of $0.22^{+0.12}_{-0.09}$ MeV and provided evidence for a sizable p-wave halo component of ^{37}Mg as revealed by a narrow momentum distribution of ^{36}Mg [12,13].

After ^{37}Mg was identified as a halo nucleus, some attempts have been made to reproduce its reaction observables. Combining the double-

* Corresponding authors.
E-mail addresses: zhangky@caep.cn (K.-Y. Zhang), zss76@buaa.edu.cn (S.-S. Zhang).

https://doi.org/10.1016/j.physletb.2023.138422
Received 1 September 2023; Received in revised form 20 December 2023; Accepted 21 December 2023
Available online 28 December 2023

folding model with the antisymmetrized molecular dynamics (AMD) model, the reaction cross sections for $^{24-36}$Mg on a C target can be mostly well reproduced, but are considerably underestimated for the case of ^{37}Mg. Even if a tail correction was added to the AMD density by using the resonating group method (RGM), an underestimation larger than 50 mb still existed for ^{37}Mg in the AMD-RGM calculations [19]. Using the Glauber model based on the Hartree-Fock-Bogoliubov (HFB) method with a phenomenological Woods-Saxon potential, Urata *et al.* could reproduce the reaction cross section for ^{37}Mg on a C target by adjusting the parameters of the depth and deformation in the potential [20]. Nevertheless, the momentum distributions of reaction fragments were not determined in the works mentioned above. Sharma *et al.* used two-set of Gaussian functions (GFs) to fit the density from the deformed relativistic mean field calculation for ^{37}Mg, and then significantly increased its diffuseness parameter so that their results from the Glauber model with this density as input agree with the experimental data of reaction cross sections and longitudinal momentum distributions [21]. As clarified in Refs. [22,23], the GFs are not suitable to describe the dilute tail part of the densities of exotic nuclei. Therefore, it is highly desirable that the reaction observables of halo nuclei can be evaluated via the structure inputs directly from microscopic models, without other adjustment.

However, a microscopic and self-consistent description of the halo in ^{37}Mg remained a challenge for nuclear structure models over years [19, 24–29]. Only in a recent Letter [30], such a description was achieved by using the deformed relativistic Hartree-Bogoliubov theory in continuum (DRHBc) [31,32], which has been successful in exploring many halo nuclei from the structure point of view, such as ^{17,19}B [14,33], ^{15,19,22}C [34,35], ^{31}Ne [22], ^{39}Na [36], and ^{42,44}Mg [31,32,37,38].

Here, we report the first unified description of the halo characteristics of ^{37}Mg from nuclear structure to reaction dynamics, by combining the DRHBc theory with the Glauber model. In Section 2, the theoretical formalism is briefly presented. Results and discussions are given in Section 3. Finally, we make a summary in Section 4.

2. Theoretical framework

Details of the DRHBc theory can be found in Refs. [32] and [39]. The starting point is the relativistic Hartree-Bogoliubov (RHB) equation, which can be solved in a Dirac Woods-Saxon basis [40,41]. Its wave function has a more reasonable asymptotic behavior compared to that of the commonly used harmonic oscillator basis and is therefore suitable for the description of weakly bound nuclei. With the density of the core nucleus and the wave function of the valence nucleon extracted from DRHBc theory, reaction observables, *i.e.*, reaction cross section and momentum distribution can be obtained by the Glauber model [42, 43].

The optical theorem [42] is utilized to obtain the reaction cross section between a projectile (P) nucleus and a target (T) nucleus, which is defined as

$$\sigma_R(P+T) = \int (1 - |e^{i\chi_{PT}(\boldsymbol{b})}|^2) d\boldsymbol{b}, \tag{1}$$

where the phase-shift function χ_{PT} is given by

$$i\chi_{PT}(\boldsymbol{b}) = -\int d\boldsymbol{r} \int d\boldsymbol{r}' \rho_P(\boldsymbol{r}) \rho_T(\boldsymbol{r}') \Gamma(\boldsymbol{b} + \boldsymbol{s} - \boldsymbol{s}'). \tag{2}$$

Here ρ is the density normalized to the mass number of a nucleus, $\int \rho(\boldsymbol{r})\, d\boldsymbol{r} = A$, $\boldsymbol{b}$ denotes the impact parameter between the projectile and the target, and $\boldsymbol{s}$ ($\boldsymbol{s}'$) refers to a two-dimensional coordinate consisting of x and y components of the projectile (target) location relative to the center-of-mass. The profile function $\Gamma(\boldsymbol{b})$ can be expressed by the nucleon-nucleon scattering amplitude $f_{NN}(\boldsymbol{q})$ as,

$$\Gamma(\boldsymbol{b}) = \frac{1}{2\pi i k_{NN}} \int e^{-i\boldsymbol{q}\cdot\boldsymbol{b}} f_{NN}(\boldsymbol{q}) d\boldsymbol{q}, \tag{3}$$

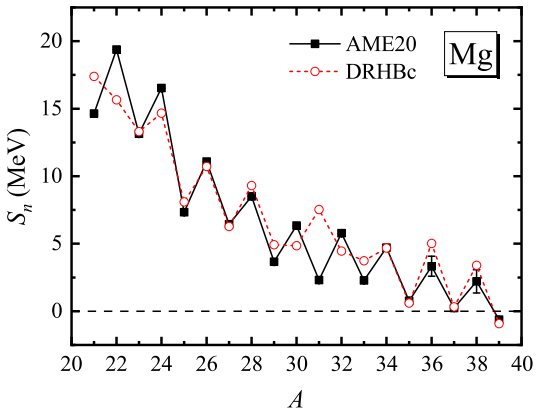

Fig. 1. One-neutron separation energy S_n as a function of mass number A for magnesium isotopes. Open red circles denote the results of the DRHBc theory. Experimental data (closed black squares) are taken from AME20 [48].

where k_{NN} denotes the nucleon momentum in the two-nucleon center-of-momentum system, and can be naturally eliminated during the integration of $i\chi_{PT}$. The phase function $i\chi_{PT}$ can be converted to the integration of the projectile (target) densities ρ_P (ρ_T) via the Fourier transforms,

$$i\chi_{PT}(b) = \int_0^\infty dq q \rho_P(q) f_{NN}(q) \rho_T(q) J_0(qb), \tag{4}$$

where q refers to the one-dimensional transferred momentum from the target to the projectile. In such a way, the projectile (target) densities ρ_P (ρ_T) can be directly provided by the DRHBc theory.

Another critical reaction observable to judge halo nuclei is the longitudinal momentum distribution of the valence nucleon and the core nucleus after one-neutron removal reaction, which is defined as [42],

$$\begin{aligned} \frac{d\sigma^{inel}_{-N}}{d\boldsymbol{P}_\parallel} &= \int d\boldsymbol{P}_\perp \frac{d\sigma^{inel}_{-N}}{d\boldsymbol{P}} = \frac{1}{2\pi\hbar} \times \\ &\int d\boldsymbol{b}_N (1 - e^{-2Im\chi_{NT}(\boldsymbol{b}_N)}) \int d\boldsymbol{s} e^{-2Im\chi_{CT}(\boldsymbol{b}_N - \boldsymbol{s})} \times \\ &\int dz \int dz' e^{\frac{i}{\hbar}\boldsymbol{P}_\parallel (z-z')} u^*_{nlj}(r') u_{nlj}(r) \frac{1}{4\pi} P_l(\hat{\boldsymbol{r}} \cdot \hat{\boldsymbol{r}}') \end{aligned} \tag{5}$$

where P_l denotes the l-order Legendre Polynomial as a function of $\boldsymbol{r} = (\boldsymbol{s}, z)$ and $\boldsymbol{r}' = (\boldsymbol{s}', z')$.

3. Results and discussions

We adopt the same numerical details as in Ref. [30] for the DRHBc calculations. It was shown in Ref. [30] that for ^{37}Mg, the bulk properties, density distributions, single-particle levels, and particularly the halo orbital and its components predicted by the different density functionals PC-F1 [44], PC-PK1 [45], NL3* [46], and PK1 [47] are consistent. Here, we only present the main results with the PC-F1 density functional to be applied in the Glauber model.

The one-neutron separation energies for magnesium isotopes by the DRHBc theory are displayed in Fig. 1, with available data from the latest atomic mass evaluation (AME20) [48]. Generally speaking, the data and the odd-even staggering are reproduced well both in trend and in magnitude, except for those close to ^{32}Mg due to the island of inversion related to the quenching of the $N = 20$ shell closure. Detailed discussion on the discrepancy between the DRHBc description and experimental data near this region can be found in Ref. [32]. On the neutron-rich side, the negative S_n of ^{39}Mg suggests ^{37}Mg as the last bound odd-N nucleus in this isotopic chain. Obviously, the small S_n of ^{37}Mg, 0.24(11) MeV [48] or $0.22^{+0.12}_{-0.09}$ MeV [12], consistent with the

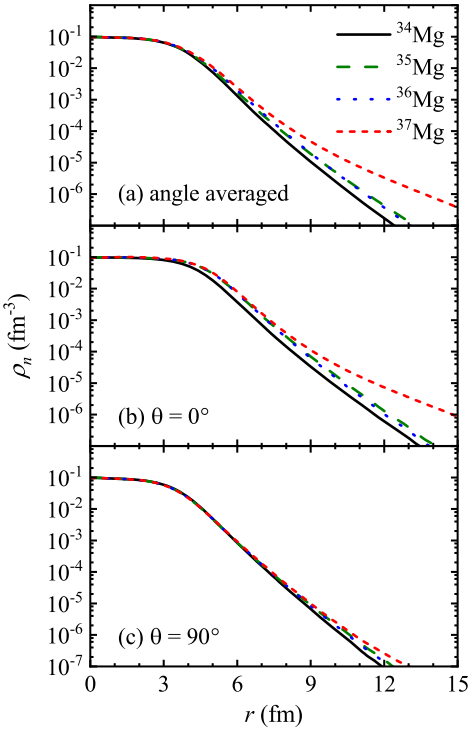

Fig. 2. (a) Angle-averaged neutron density distribution, (b) the neutron density distribution along the symmetry axis, and (c) the neutron density distribution perpendicular to the symmetry axis for $^{34-37}$Mg in the DRHBc calculations.

predicted 0.32 MeV from the DRHBc theory [30], is one of the signals for a one-neutron halo in this nucleus.

We plot neutron density profiles of $^{34-37}$Mg in Fig. 2, which are the input for the Glauber model. The neutron density distributions along ($\theta = 0°$) and perpendicular to ($\theta = 90°$) the symmetry axis are respectively exhibited in Figs. 2(b) and 2(c), where θ represents the angle of deviation from the symmetry axis. In Fig. 1 of Ref. [30], the neutron densities are shown in the xz plane with z being the symmetry axis. Hence, Figs. 2(b) and 2(c) here correspond to the neutron density distributions along the central vertical (z axis) and horizontal (x axis) lines in Fig. 1 of Ref. [30], respectively. To examine the overall evolution trend, we average the neutron densities in different directions and obtain the angle-averaged results depicted in Fig. 2(a). The angle-averaged neutron density of ^{37}Mg extends far from the center of the nucleus with a long and dilute tail, supporting its neutron halo structure. By comparing Figs. 2(b) and 2(c), one can realize that the halo is formed mainly along the symmetry axis, which indicates that the shape of the halo is prolate, the same as the core with $\beta_2 = 0.46$ [30]. This implies that ^{37}Mg is a deformed halo nucleus without the quadrupole shape decoupling as predicted in ^{42,44}Mg [31,32]. The neutron root-mean-square (rms) radii calculated from neutron densities are respectively 3.60, 3.66, and 3.77 fm for ^{35}Mg, ^{36}Mg, and ^{37}Mg. The neutron halo of ^{37}Mg is further supported by the remarkable increment of the neutron rms radius from ^{36}Mg to ^{37}Mg, which is nearly twice that from ^{35}Mg to ^{36}Mg.

While the density distributions are not readily measurable, they can serve as inputs for the Glauber model to calculate the reaction observables which can then be directly compared with measured data. We calculate the reaction cross sections σ_R of $^{20-37}$Mg bombarding a C target at 240 MeV/nucleon by Eq. (1). The results (open red circles) are plotted in Fig. 3, together with the AMD/AMD-RGM calculations (blue open/closed squares) and compared with available data (closed circles) [13]. Since the difference between reaction and interaction cross sections for inelastic reactions is negligible at 240 MeV/nucleon [13], here we do not distinguish them. It can be seen that most of our predictions are in satisfactory agreement with the experimental data within

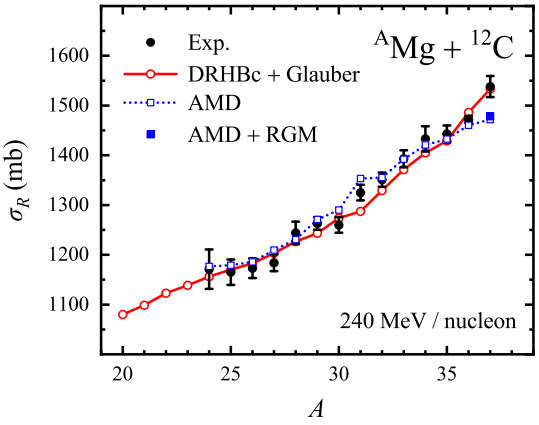

Fig. 3. Reaction cross sections σ_R of $^{20-37}$Mg bombarding a C target at 240 MeV/nucleon. Open red circles stand for our predictions with the Glauber model with inputs from the DRHBc theory. Open/closed blue squares stand for the results from the AMD/AMD-RGM approach [19]. Experimental data (closed black circles) are taken from Ref. [13] for comparison.

1σ uncertainty, showing the validity of the DRHBc + Glauber approach. In particular, without any artificial adjustment or introducing free parameters, the large reaction cross section of the halo nucleus ^{37}Mg on a C target is reproduced, demonstrating the advantage of our approach over previous works [13,19–21]. Hence, this is the first time to successfully describe the reaction cross section of ^{37}Mg on a C target starting purely from microscopic structure inputs.

One can also find in Fig. 3 that a kink at ^{31}Mg is not reproduced and the reaction cross sections for $^{31-34}$Mg are underestimated by the DRHBc + Glauber approach. This is related to the fact that the mean-field descriptions [49–51] can hardly reproduce the large deformations of the magnesium isotopes located in the island of inversion near $N = 20$. From the measured $B(E2: 0_1^+ \rightarrow 2_1^+)$ values, the extracted deformations for ^{30,32,34}Mg are respectively $\beta_2 = 0.42$, 0.50, and 0.55 [52]. However, the ground-state deformations for $^{30-34}$Mg are respectively $\beta_2 = 0.00$, -0.08, 0.00, 0.16, and 0.25 from the present DRHBc calculations and are $\beta_2 = 0.29$, 0.44, 0.40, 0.44, and 0.35 predicted by the AMD model [19]. Although both the DRHBc and the AMD approaches fail to exactly reproduce the experimental values, the larger deformations in the AMD model lead to larger reaction cross sections, reproducing better the measured results for $^{31-34}$Mg. The deformation increases significantly from $\beta_2 = 0.29$ of ^{30}Mg to $\beta_2 = 0.44$ of ^{31}Mg in the AMD calculations, which might be responsible for the kink of the reaction cross section at ^{31}Mg, but this is not the case in the DRHBc calculations.

As another visualized quantity, the longitudinal momentum distributions for ^{34,36}Mg residues after one-neutron removal from ^{35,37}Mg bombarding a C target at 240 MeV/nucleon are calculated by Eq. (5) with a Lorentzian folded with the same experimental resolution 31 MeV/c as that used in Ref. [53]. Our predictions are displayed in Fig. 4 and compared with the experimental data [12]. The momentum distribution for ^{36}Mg residues shows a narrow peak shape, and agrees well with the measured data [12]. It can be clearly seen from Fig. 4 that the contribution (red dashed line) from p wave dominates, while the contribution (blue dashed-dotted line) from f wave widens the momentum distribution for the breakup reaction of ^{37}Mg on a C target. As listed in Table I of Ref. [30], the main components of the weakly bound orbital occupied by the halo neutron are 38% for $2p_{1/2}$, 19% for $2p_{3/2}$, 6% for $1f_{5/2}$, and 32% for $1f_{7/2}$. The narrower momentum distribution can be explained by the larger p-wave components in the DRHBc calculations [30], which is comparable to the $\approx 40\%$ p-wave occupancy suggested in Ref. [12]. Since the momentum resolution for ^{34}Mg residues after the breakup reaction of ^{35}Mg on ^{12}C is not available from experiment, we adopt the same value as that in the calculations for ^{36}Mg. We can see from Fig. 4 that the calculated momentum distri-

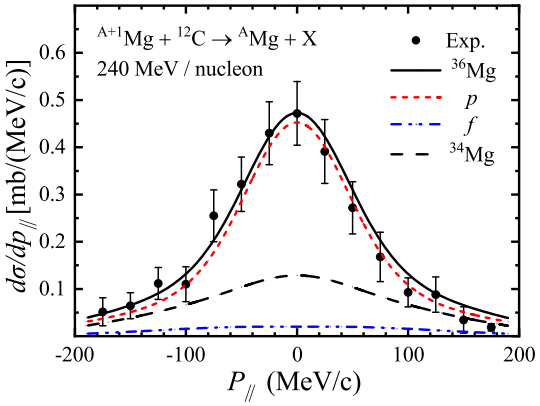

Fig. 4. Inclusive longitudinal momentum distributions of ^{34,36}Mg residues after one-neutron removal reaction of ^{35,37}Mg bombarding a C target at 240 MeV/nucleon. The black solid/dashed line refers to the predictions for ^{36}Mg/^{34}Mg with the DRHBc + Glauber approach. The red dashed line and blue dash-dotted line denote the individual contributions to the results for ^{36}Mg from p- and f-wave neutron removal, respectively. Experimental data for the ^{37}Mg reaction are taken from Ref. [12].

bution for ^{34}Mg residues is much flatter than that for ^{36}Mg residues, in agreement with the Heisenberg uncertainty principle. Quantitatively, the peak value of the momentum distribution for ^{36}Mg residues is 3.69 times larger than that for ^{34}Mg residues, and the extracted full widths at half maximum (FWHM) are approximately 132 MeV/c and 207 MeV/c, respectively. These differences are due to only $\approx 10\%$ p-wave components of the valence neutron in ^{35}Mg and its tightly bound (non-halo) structure. The FWHM of our predictions before convolution is 82 MeV/c (130 MeV/c) for ^{36}Mg (^{34}Mg) residues, which is consistent with 82(13) MeV/c obtained in Ref. [12]. Therefore, the narrow momentum distribution observed in the one-neutron removal reaction of ^{37}Mg as direct evidence for its halo structure can be well reproduced by the DRHBc + Glauber approach and therefore well explained by our microscopic nuclear structure framework.

4. Summary

In this paper, we have given the first unified description of the halo nucleus ^{37}Mg from the microscopic structure to reaction observables. Firstly, one-neutron separation energies of $^{20-37}$Mg and the extended neutron density distribution of ^{37}Mg are well described by the DRHBc theory. Secondly, the density of the core nucleus and the wave function of the valence nucleon from the DRHBc theory are adopted as microscopic inputs for the Glauber reaction model to study the reaction observables of neutron-rich magnesium isotopes on C targets with 240 MeV/nucleon beams.

Most of the calculated reaction cross sections are in satisfactory agreement with the experimental data within 1σ uncertainty. In particular, the large reaction cross section for the ^{37}Mg reaction is well reproduced without any adjustment. The slope of the reaction cross sections from ^{36}Mg to ^{37}Mg are significantly enhanced by a factor of two compared to that from ^{34}Mg to ^{35}Mg.

We further study the longitudinal momentum distributions of ^{34,36}Mg residues after one-neutron removal reaction of ^{35,37}Mg on C targets. It turns out that our predicted longitudinal momentum distribution for ^{36}Mg residues agrees well with measured data, showing a peak much narrower than its neighbors, in agreement with the Heisenberg uncertainty principle. This narrow momentum distribution can be self-consistently interpreted as being caused by the dominant p-wave components of the valence neutron. Therefore, for the first time, a unified description of the halo features of ^{37}Mg is achieved from nuclear structure to reaction dynamics.

Declaration of competing interest

The authors declare that they have no known competing financial interests or personal relationships that could have appeared to influence the work reported in this paper.

Data availability

Data will be made available on request.

Acknowledgements

We appreciate the discussion with Professors De-Qing Fang and Zai-Hong Yang, thank Professor Michael Smith for his careful reading of this manuscript, and thank Hao-Chen Li for his careful checking of the data, Rui-Jie Liang and Li-Yang Wang for their attempts on the spherical case also. This work was supported by the National Natural Science Foundation of China (Grant Nos. 12175010, 12305125, U2230207, U2030209, 11935003, 11975031, 12141501, and 12070131001) and the National Key R&D Program of China (Grant Nos. 2020YFA0406001 and 2020YFA0406002). Part of the results described in this work were obtained using High-performance computing Platform of Peking University.

References

[1] J. Al-Khalili, E. Roeckl, An Introduction to Halo Nuclei, Springer, Berlin Heidelberg, 2004, pp. 77–112 (Chapter 3), https://doi.org/10.1007/978-3-540-44490-9_3.
[2] A. Jensen, K. Riisager, D. Fedorov, E. Garrido, Structure and reactions of quantum halos, Rev. Mod. Phys. 76 (1) (2004) 215–261, https://doi.org/10.1103/RevModPhys.76.215.
[3] P. Hansen, B. Jonson, The neutron halo of extremely neutron-rich nuclei, Europhys. Lett. 4 (4) (1987) 409, https://doi.org/10.1209/0295-5075/4/4/005.
[4] P. Ring, Relativistic mean field theory in finite nuclei, Prog. Part. Nucl. Phys. 37 (1996) 193–263, https://doi.org/10.1016/0146-6410(96)00054-3.
[5] S.-S. Zhang, M.S. Smith, Z.-S. Kang, J. Zhao, Microscopic self-consistent study of neon halos with resonant contributions, Phys. Lett. B 730 (2014) 30–35, https://doi.org/10.1016/j.physletb.2014.01.023.
[6] X.-F. Li, D.-Q. Fang, Y.-G. Ma, Determination of the neutron skin thickness from interaction cross section and charge-changing cross section for B, C, N, O, F isotopes, Nucl. Sci. Tech. 27 (2016) 71, https://doi.org/10.1007/s41365-016-0064-z.
[7] S.-Z. Xu, S.-S. Zhang, X.-Q. Jiang, M.S. Smith, The complex momentum representation approach and its application to low-lying resonances in ^{17}O and ^{29,31}F, Nucl. Sci. Tech. 34 (2023) 5, https://doi.org/10.1007/s41365-022-01159-y.
[8] K.Y. Zhang, S.Q. Zhang, J. Meng, Possible neutron halo in the triaxial nucleus ^{42}Al, Phys. Rev. C 108 (2023) L041301, https://doi.org/10.1103/PhysRevC.108.L041301.
[9] I. Tanihata, H. Savajols, R. Kanungo, Recent experimental progress in nuclear halo structure studies, Prog. Part. Nucl. Phys. 68 (2013) 215–313, https://doi.org/10.1016/j.ppnp.2012.07.001.
[10] T. Nakamura, Coulomb Breakup and Soft E1 Excitation of Neutron Halo Nuclei, Springer Nature, Singapore, 2020, pp. 1–37, https://doi.org/10.1007/978-981-15-8818-1_68-1.
[11] I. Tanihata, H. Hamagaki, O. Hashimoto, Y. Shida, N. Yoshikawa, K. Sugimoto, O. Yamakawa, T. Kobayashi, N. Takahashi, Measurements of interaction cross sections and nuclear radii in the light p-shell region, Phys. Rev. Lett. 55 (24) (1985) 2676, https://doi.org/10.1103/PhysRevLett.55.2676.
[12] N. Kobayashi, T. Nakamura, Y. Kondo, J.A. Tostevin, Y. Utsuno, N. Aoi, H. Baba, R. Barthelemy, M.A. Famiano, N. Fukuda, N. Inabe, M. Ishihara, R. Kanungo, S. Kim, T. Kubo, G.S. Lee, H.S. Lee, M. Matsushita, T. Motobayashi, T. Ohnishi, N.A. Orr, H. Otsu, T. Otsuka, T. Sako, H. Sakurai, Y. Satou, T. Sumikama, H. Takeda, S. Takeuchi, R. Tanaka, Y. Togano, K. Yoneda, Observation of a p-wave one-neutron halo configuration in ^{37}Mg, Phys. Rev. Lett. 112 (2014) 242501, https://doi.org/10.1103/PhysRevLett.112.242501.
[13] M. Takechi, S. Suzuki, D. Nishimura, M. Fukuda, T. Ohtsubo, M. Nagashima, T. Suzuki, T. Yamaguchi, A. Ozawa, T. Moriguchi, et al., Evidence of halo structure in ^{37}Mg observed via reaction cross sections and intruder orbitals beyond the island of inversion, Phys. Rev. C 90 (6) (2014) 061305, https://doi.org/10.1103/PhysRevC.90.061305.
[14] Z.H. Yang, Y. Kubota, A. Corsi, K. Yoshida, X.-X. Sun, J.G. Li, M. Kimura, N. Michel, K. Ogata, C.X. Yuan, Q. Yuan, G. Authelet, H. Baba, C. Caesar, D. Calvet, A. Delbart, M. Dozono, J. Feng, F. Flavigny, J.-M. Gheller, J. Gibelin, A. Giganon, A. Gillibert, K. Hasegawa, T. Isobe, Y. Kanaya, S. Kawakami, D. Kim, Y. Kiyokawa, M. Kobayashi, N. Kobayashi, T. Kobayashi, Y. Kondo, Z. Korkulu, S. Koyama, V. Lapoux, Y. Maeda, F.M. Marqués, T. Motobayashi, T. Miyazaki, T. Nakamura, N. Nakatsuka, Y. Nishio,

A. Obertelli, A. Ohkura, N.A. Orr, S. Ota, H. Otsu, T. Ozaki, V. Panin, S. Paschalis, E.C. Pollacco, S. Reichert, J.-Y. Roussé, A.T. Saito, S. Sakaguchi, M. Sako, C. Santamaria, M. Sasano, H. Sato, M. Shikata, Y. Shimizu, Y. Shindo, L. Stuhl, T. Sumikama, Y.L. Sun, M. Tabata, Y. Togano, J. Tsubota, F.R. Xu, J. Yasuda, K. Yoneda, J. Zenihiro, S.-G. Zhou, W. Zuo, T. Uesaka, Quasifree neutron knockout reaction reveals a small s-orbital component in the borromean nucleus ^{17}B, Phys. Rev. Lett. 126 (2021) 082501, https://doi.org/10.1103/PhysRevLett.126.082501.

[15] D.S. Ahn, J. Amano, H. Baba, N. Fukuda, H. Geissel, N. Inabe, S. Ishikawa, N. Iwasa, T. Komatsubara, T. Kubo, K. Kusaka, D.J. Morrissey, T. Nakamura, M. Ohtake, H. Otsu, T. Sakakibara, H. Sato, B.M. Sherrill, Y. Shimizu, T. Sumikama, H. Suzuki, H. Takeda, O.B. Tarasov, H. Ueno, Y. Yanagisawa, K. Yoshida, Discovery of ^{39}Na, Phys. Rev. Lett. 129 (2022) 212502, https://doi.org/10.1103/PhysRevLett.129.212502.

[16] M. Thoennessen, Plans for the facility for rare isotope beams, Nucl. Phys. A 834 (1–4) (2010) 688c–693c, https://doi.org/10.1016/j.nuclphysa.2010.01.125.

[17] H.L. Crawford, V. Tripathi, J.M. Allmond, B.P. Crider, R. Grzywacz, S.N. Liddick, A. Andalib, E. Argo, C. Benetti, S. Bhattacharya, C.M. Campbell, M.P. Carpenter, J. Chan, A. Chester, J. Christie, B.R. Clark, I. Cox, A.A. Doetsch, J. Dopfer, J.G. Duarte, P. Fallon, A. Frotscher, T. Gaballah, T.J. Gray, J.T. Harke, J. Heideman, H. Heugen, R. Jain, T.T. King, N. Kitamura, K. Kolos, F.G. Kondev, A. Laminack, B. Longfellow, R.S. Lubna, S. Luitel, M. Madurga, R. Mahajan, M.J. Mogannam, C. Morse, S. Neupane, A. Nowicki, T.H. Ogunbeku, W.-J. Ong, C. Porzio, C.J. Prokop, B.C. Rasco, E.K. Ronning, E. Rubino, T.J. Ruland, K.P. Rykaczewski, L. Schaedig, D. Seweryniak, K. Siegl, M. Singh, S.L. Tabor, T.L. Tang, T. Wheeler, J.A. Winger, Z. Xu, Crossing N = 28 toward the neutron drip line: first measurement of half-lives at FRIB, Phys. Rev. Lett. 129 (2022) 212501, https://doi.org/10.1103/PhysRevLett.129.212501.

[18] T.J. Gray, J.M. Allmond, Z. Xu, T.T. King, R.S. Lubna, H.L. Crawford, V. Tripathi, B.P. Crider, R. Grzywacz, S.N. Liddick, A.O. Macchiavelli, T. Miyagi, A. Poves, A. Andalib, E. Argo, C. Benetti, S. Bhattacharya, C.M. Campbell, M.P. Carpenter, J. Chan, A. Chester, J. Christie, B.R. Clark, I. Cox, A.A. Doetsch, J. Dopfer, J.G. Duarte, P. Fallon, A. Frotscher, T. Gaballah, J.T. Harke, J. Heideman, H. Huegen, J.D. Holt, R. Jain, N. Kitamura, K. Kolos, F.G. Kondev, A. Laminack, B. Longfellow, S. Luitel, M. Madurga, R. Mahajan, M.J. Mogannam, C. Morse, S. Neupane, A. Nowicki, T.H. Ogunbeku, W.-J. Ong, C. Porzio, C.J. Prokop, B.C. Rasco, E.K. Ronning, E. Rubino, T.J. Ruland, K.P. Rykaczewski, L. Schaedig, D. Seweryniak, K. Siegl, M. Singh, A.E. Stuchbery, S.L. Tabor, T.L. Tang, T. Wheeler, J.A. Winger, J.L. Wood, Microsecond isomer at the N = 20 island of shape inversion observed at FRIB, Phys. Rev. Lett. 130 (2023) 242501, https://doi.org/10.1103/PhysRevLett.130.242501.

[19] S. Watanabe, K. Minomo, M. Shimada, S. Tagami, M. Kimura, M. Takechi, M. Fukuda, D. Nishimura, T. Suzuki, T. Matsumoto, et al., Ground-state properties of neutron-rich Mg isotopes, Phys. Rev. C 89 (4) (2014) 044610, https://doi.org/10.1103/PhysRevC.89.044610.

[20] Y. Urata, K. Hagino, H. Sagawa, Role of deformation in odd-even staggering in reaction cross sections for ^{30,31,32}Ne and ^{36,37,38}Mg isotopes, Phys. Rev. C 96 (6) (2017) 064311, https://doi.org/10.1103/PhysRevC.96.064311.

[21] M.K. Sharma, R. Panda, M.K. Sharma, S. Patra, Search for halo structure in ^{37}Mg using the Glauber model and microscopic relativistic mean-field densities, Phys. Rev. C 93 (1) (2016) 014322, https://doi.org/10.1103/PhysRevC.93.014322.

[22] S.S. Zhang, S.Y. Zhong, B. Shao, M.S. Smith, Self-consistent description of the halo nature of ^{31}Ne with continuum and pairing correlations, J. Phys. G, Nucl. Part. Phys. 49 (2) (2022) 025102, https://doi.org/10.1088/1361-6471/ac430e.

[23] S.Y. Zhong, S.S. Zhang, X.X. Sun, M.S. Smith, Study of the deformed halo nucleus ^{31}Ne with Glauber model based on microscopic self-consistent structures, Sci. China, Phys. Mech. Astron. 65 (6) (2022) 1–9, https://doi.org/10.1007/s11433-022-1894-6.

[24] X.-D. Xu, S.-S. Zhang, A.J. Signoracci, M.S. Smith, Z.P. Li, Analytical continuation from bound to resonant states in the Dirac equation with quadrupole-deformed potentials, Phys. Rev. C 92 (2) (2015) 024324, https://doi.org/10.1103/physrevc.92.024324.

[25] X.-Y. Xiong, J.-C. Pei, Y.-N. Zhang, Y. Zhu, Study of weakly-bound odd-A nuclei with quasiparticle blocking*, Chin. Phys. C 40 (2) (2016) 024101, https://doi.org/10.1088/1674-1137/40/2/024101.

[26] H. Nakada, K. Takayama, Intertwined effects of pairing and deformation on neutron halos in magnesium isotopes, Phys. Rev. C 98 (2018) 011301, https://doi.org/10.1103/PhysRevC.98.011301.

[27] H. Kasuya, K. Yoshida, Hartree–Fock–Bogoliubov theory for odd-mass nuclei with a time-odd constraint and application to deformed halo nuclei, Prog. Theor. Exp. Phys. 2021 (1) (11 2020) 013D01, https://doi.org/10.1093/ptep/ptaa163.

[28] T.-T. Sun, L. Qian, C. Chen, P. Ring, Z. Li, et al., Green's function method for the single-particle resonances in a deformed Dirac equation, Phys. Rev. C 101 (1) (2020) 014321, https://doi.org/10.1103/PHYSREVC.101.014321.

[29] V. Choudhary, W. Horiuchi, M. Kimura, R. Chatterjee, Enormous nuclear surface diffuseness of Ne and Mg isotopes in the island of inversion, Phys. Rev. C 104 (2021) 054313, https://doi.org/10.1103/PhysRevC.104.054313.

[30] K. Zhang, S. Yang, J. An, S. Zhang, P. Papakonstantinou, M.-H. Mun, Y. Kim, H. Yan, Missed prediction of the neutron halo in ^{37}Mg, Phys. Lett. B 844 (2023) 138112, https://doi.org/10.1016/j.physletb.2023.138112.

[31] S.-G. Zhou, J. Meng, P. Ring, E.-G. Zhao, Neutron halo in deformed nuclei, Phys. Rev. C 82 (2010) 011301(R), https://doi.org/10.1103/PhysRevC.82.011301.

[32] L. Li, J. Meng, P. Ring, E.-G. Zhao, S.-G. Zhou, Deformed relativistic Hartree-Bogoliubov theory in continuum, Phys. Rev. C 85 (2012) 024312, https://doi.org/10.1103/PhysRevC.85.024312.

[33] X.-X. Sun, Deformed two-neutron halo in ^{19}B, Phys. Rev. C 103 (2021) 054315, https://doi.org/10.1103/PhysRevC.103.054315.

[34] X.-X. Sun, J. Zhao, S.-G. Zhou, Shrunk halo and quenched shell gap at N = 16 in ^{22}C: inversion of sd states and deformation effects, Phys. Lett. B 785 (2018) 530, https://doi.org/10.1016/j.physletb.2018.08.071.

[35] X.-X. Sun, J. Zhao, S.-G. Zhou, Study of ground state properties of carbon isotopes with deformed relativistic Hartree-Bogoliubov theory in continuum, Nucl. Phys. A 1003 (2020) 122011, https://doi.org/10.1016/j.nuclphysa.2020.122011.

[36] K.Y. Zhang, P. Papakonstantinou, M.-H. Mun, Y. Kim, H. Yan, X.-X. Sun, Collapse of the N = 28 shell closure in the newly discovered ^{39}Na nucleus and the development of deformed halos towards the neutron dripline, Phys. Rev. C 107 (2023) L041303, https://doi.org/10.1103/PhysRevC.107.L041303.

[37] K.Y. Zhang, D.Y. Wang, S.Q. Zhang, Effects of pairing, continuum, and deformation on particles in the classically forbidden regions for Mg isotopes, Phys. Rev. C 100 (2019) 034312, https://doi.org/10.1103/PhysRevC.100.034312.

[38] X.-X. Sun, S.-G. Zhou, Rotating deformed halo nuclei and shape decoupling effects, Sci. Bull. 66 (20) (2021) 2072–2078, https://doi.org/10.1016/j.scib.2021.07.005.

[39] K. Zhang, M.-K. Cheoun, Y.-B. Choi, P.S. Chong, J. Dong, L. Geng, E. Ha, X. He, C. Heo, M.C. Ho, E.J. In, S. Kim, Y. Kim, C.-H. Lee, J. Lee, Z. Li, T. Luo, J. Meng, M.-H. Mun, Z. Niu, C. Pan, P. Papakonstantinou, X. Shang, C. Shen, G. Shen, W. Sun, X.-X. Sun, C.K. Tam Thaivayongnou, C. Wang, S.H. Wong, X. Xia, Y. Yan, R.W.-Y. Yeung, T.C. Yiu, S. Zhang, W. Zhang, S.-G. Zhou, Deformed relativistic Hartree-Bogoliubov theory in continuum with a point-coupling functional: examples of even-even Nd isotopes, Phys. Rev. C 102 (2020) 024314, https://doi.org/10.1103/PhysRevC.102.024314.

[40] S.-G. Zhou, J. Meng, P. Ring, Spherical relativistic Hartree theory in a Woods-Saxon basis, Phys. Rev. C 68 (2003) 034323, https://doi.org/10.1103/PhysRevC.68.034323.

[41] K.Y. Zhang, C. Pan, S.Q. Zhang, Optimized Dirac Woods-Saxon basis for covariant density functional theory, Phys. Rev. C 106 (2022) 024302, https://doi.org/10.1103/PhysRevC.106.024302.

[42] B. Abu-Ibrahim, Y. Ogawa, Y. Suzuki, I. Tanihata, Cross section calculations in Glauber model: I. core plus one-nucleon case, Comput. Phys. Commun. 151 (3) (2003) 369–386, https://doi.org/10.1016/S0010-4655(02)00734-8.

[43] R. Glauber, Lectures in Theoretical Physics, Interscience Publishers, New York, 1959.

[44] T. Bürvenich, D.G. Madland, J.A. Maruhn, P.-G. Reinhard, Nuclear ground state observables and QCD scaling in a refined relativistic point coupling model, Phys. Rev. C 65 (2002) 044308, https://doi.org/10.1103/PhysRevC.65.044308.

[45] P.W. Zhao, Z.P. Li, J.M. Yao, J. Meng, New parametrization for the nuclear covariant energy density functional with a point-coupling interaction, Phys. Rev. C 82 (2010) 054319, https://doi.org/10.1103/PhysRevC.82.054319.

[46] G.A. Lalazissis, S. Karatzikos, R. Fossion, D.P. Arteaga, A.V. Afanasjev, P. Ring, The effective force NL3 revisited, Phys. Lett. B 671 (1) (2009) 36–41, https://doi.org/10.1016/j.physletb.2008.11.070.

[47] W. Long, J. Meng, N. Van Giai, S.-G. Zhou, New effective interactions in relativistic mean field theory with nonlinear terms and density-dependent meson-nucleon coupling, Phys. Rev. C 69 (2004) 034319, https://doi.org/10.1103/PhysRevC.69.034319.

[48] M. Wang, W.J. Huang, F.G. Kondev, G. Audi, S. Naimi, The AME 2020 atomic mass evaluation II. tables, graphs and references, Chin. Phys. C 45 (3) (2021) 030003, https://doi.org/10.1088/1674-1137/abddaf.

[49] Z. Ren, Z. Zhu, Y. Cai, G. Xu, Relativistic mean-field study of mg isotopes, Phys. Lett. B 380 (3) (1996) 241–246, https://doi.org/10.1016/0370-2693(96)00462-5, https://www.sciencedirect.com/science/article/pii/0370269396004625.

[50] G.A. Lalazissis, S. Raman, P. Ring, Ground-state properties of even-even nuclei in the relativistic mean-field theory, At. Data Nucl. Data Tables 71 (1) (1999) 1–40, https://doi.org/10.1006/adnd.1998.0795, https://www.sciencedirect.com/science/article/pii/S0092640X98907951.

[51] K. Zhang, M.-K. Cheoun, Y.-B. Choi, P.S. Chong, J. Dong, Z. Dong, X. Du, L. Geng, E. Ha, X.-T. He, C. Heo, M.C. Ho, E.J. In, S. Kim, Y. Kim, C.-H. Lee, J. Lee, H. Li, Z. Li, T. Luo, J. Meng, M.-H. Mun, Z. Niu, C. Pan, P. Papakonstantinou, X. Shang, C. Shen, G. Shen, W. Sun, X.-X. Sun, C.K. Tam Thaivayongnou, C. Wang, X. Wang, S.H. Wong, J. Wu, X. Wu, X. Xia, Y. Yan, R.W.-Y. Yeung, T.C. Yiu, S. Zhang, W. Zhang, X. Zhang, Q. Zhao, S.-G. Zhou, Nuclear mass table in deformed relativistic Hartree–Bogoliubov theory in continuum, i: even–even nuclei, At. Data Nucl. Data Tables 144 (2022) 101488, https://doi.org/10.1016/j.adt.2022.101488, https://www.sciencedirect.com/science/article/pii/S0092640X22000018.

[52] B. Pritychenko, M. Birch, B. Singh, M. Horoi, Tables of e2 transition probabilities from the first 2+ states in even–even nuclei, At. Data Nucl. Data Tables 107 (2016) 1–139, https://doi.org/10.1016/j.adt.2015.10.001, https://www.sciencedirect.com/science/article/pii/S0092640X15000406.

[53] N. Kobayashi, Ph.D. thesis, Department of Physics, Graduate School of Science and Engineering, Tokyo Institute of Technology, 2013.